

Object-Specific and Target-Free Procedure for the Color Accuracy of a Two-Dimensional Digital Reproduction

M. Selva and L. Stefani

Institute of Applied Physics, “N. Carrara” Via Madonna del Piano 10, 50019 Sesto Fiorentino (FI), Italy
E-mail: m.selva@ifac.cnr.it

G. Trumpy

Imaging & Media Lab, University of Basel, Bernoullistrasse 32, CH-4056 Basel, Switzerland

Abstract. This article presents a new methodology for the color accuracy optimization of a two-dimensional digital reproduction. Selecting a training set referring to the colorimetric content of the object to be reproduced results in a significant improvement of the color accuracy of an RGB reproduction. Some authors have developed methodologies for color accuracy optimization that involve the creation of specific custom-made reference targets. The methodology presented here does not involve the creation of custom-made targets, as the reference colors are selected directly on the object. In fact, a clusterization is performed on the RGB image of the object and a set of representative colors is achieved. For each RGB representative color, the corresponding CIELAB value is measured and a training set is obtained that can be used to define a transformation that maps all RGB values into CIELAB values. The experiments conducted show that using this methodology considerably improves color accuracy. © 2011 Society for Imaging Science and Technology. [DOI: 10.2352/J.ImagingSci.Technol.2011.55.6.060503]

INTRODUCTION

Digital Color Accuracy

The acquisition of a color image that reproduces the appearance of a certain object consists in coding the radiance into three output values. The colorimetric characterization of an image acquisition device is a process designed to provide the correspondence between the values recorded by the device and the encoded CIE colorimetric values. The identification of this correspondence can be made with different methods; e.g., three-dimensional look-up-tables,¹ polynomial modeling,² and neural networks.³ The result is a transformation between the three-dimensional space (RGB) of the device (*device-dependent*) and a CIE color space (*device-independent*). This transformation is generally encoded in the metadata *ICC profile*. Through this metadata, the digital images can provide precise color information.⁴

For the identification of the optimal transformation, a set of experimental data is necessary (*training set*); i.e., a set of correspondences between the device-dependent values and the device-independent values. Generally, these experi-

mental data are collected by acquiring the image of specific targets, whose spectral reflectances are known.

An accurate digital reproduction provides the match between the appearance of the colors of the object and the appearance of the colors of its reproduction. Focusing the attention on images that reproduce plane surfaces that are uniformly illuminated (hence *reproductions*), and considering the perceptual differences in simplified observing conditions, it is proper to use the CIELAB space (defined here with the illuminant D50 and the observer CIE1931) and the metric ΔE . In this article, the color accuracy of an RGB reproduction equals the closeness between the CIELAB values obtained through rigorous spectral measurements performed on the object and those obtained through its digital RGB acquisition (*colorimetric accuracy*).

The optimization of color accuracy can follow two different approaches: accomplishing the complete color characterization of the device that produced the image (*general characterization*), thereby obtaining a transformation valid for each color to be reproduced; or, otherwise, carrying out a procedure developed in order to obtain the best possible result for the specific case of the object under consideration (*object-specific optimization*). The object-specific optimization is discussed below.

Object-Specific Methodology

The greatest strength of object-specific methodology lies in considering the most appropriate target; however, for this very reason, the transformation found is only valid for the object being considered or for objects with similar color characteristics. This is mostly true when dealing with objects with restricted color distribution.

In order to perform a specific optimization, the training set should be a significantly representative selection of the colors that have to be reproduced in the digital image. This selection is critical.^{5,6} The various test charts available on the market (e.g., ColorChecker®, IT8, etc.) are used to perform a general characterization of the device and, therefore, are unsuitable for a specific optimization. Their colors, in fact, have to be representative of a generic chromatic content and, for this reason, the CIELAB values are

Received Feb. 10, 2011; accepted for publication Oct. 7, 2011; published online Dec. 22, 2011

1062-3701/2011/55(6)/060503-1/9/\$20.00.

distributed in the whole colorimetric space, so that significant volumes of it left uncovered are not too large.

A possible approach is to physically create a custom-made target by selecting the patches from a standard color sample book⁷ referring to the colorimetric characteristics of the specific object.

For this purpose, it is important to point out that the human visual system shows properties of metamerism that are different from those of an imaging device. In fact, the imaging device is characterized by three specific spectral sensitivities $r(\lambda)$, $g(\lambda)$, $b(\lambda)$, while the human visual system is coded by the CIE *color matching functions* (CMFs) $\bar{x}(\lambda)$, $\bar{y}(\lambda)$, $\bar{z}(\lambda)$.⁸ The exact reproduction of color would be possible only if these spectral sensitivities are a linear combination of the CMFs⁹ (*Luther-Ives conditions*¹⁰). However, generally, the spectral sensitivities of an RGB acquisition device do not satisfy this request. Therefore, colors exist with different reflectance spectra and different CIELAB values that, under certain conditions, result in the same recorded RGB value (*metamer mismatch*¹¹). This fact results in negative effects on the performances of the color optimization of digital reproductions.^{12,13}

That being so, some authors¹⁴ have presented a procedure for creating accurate digital reproductions that uses a specially created color target constituted by the same type of materials that characterizes the object; in particular, in order to correctly reproduce *gouache* paintings, they created a color target with the same painting technique.

Even though these approaches provide a real improvement in the performance of the optimization, they are very time-consuming and several difficulties may be encountered in the creation of the custom target. This article, therefore, proposes and validates a methodology that does not require the creation of a target.

A Target-Free Methodology

The methodology presented in this article performs an optimization specific to the object to be reproduced and does not require the physical creation of a specific target, preventing the problems related to its creation. This methodology requires the identification of a training set of colors representative of the object. The colors of this set are selected among those of the object itself. A set composed of the RGB values of the object and their corresponding reference CIELAB values constitutes the training set of the procedure.

Since the training set is a sampling of points of the object itself, by adopting this approach, the required analogy¹² between the type of material that constitutes the training set and the type of material that constitutes the object to be reproduced is obviously perfect.

The next section describes in detail the issues related to the spectrophotometric reflectance measurements needed.

SPECTROPHOTOMETRIC REFLECTANCE MEASUREMENTS

As stated in the Introduction, carrying out the methodology presented in this article necessitates the CIELAB values

of a selection of specific points of the object. A spot colorimeter is an effective means of obtaining those data. Its use would be sufficient in the application context, but for the purposes of studying, defining, and validating the new methodology, the spot measurements alone are not sufficient. In fact, they can certainly be used to define the transformation from the device-dependent space to the device-independent one, but they do not allow computation of the colorimetric accuracy of all the pixels of the image after the application of the transformation. To this end, the CIELAB values of the points of the object corresponding to all the pixels of the RGB image have to be measured.

Imaging Spectroscopy

The CIELAB values can be obtained with *imaging spectroscopy*. From the reflectance spectrum, using the CIE calculations, it is possible to derive the corresponding CIELAB values of the acquired object.⁸

According to the spectral resolution needed, different devices can be used, i.e., multispectral and hyper-spectral scanners. As an example, an interesting multispectral scanner based on LED technology is described in the literature.¹⁵

In this experiment, due to the necessity of a high spectral resolution, we adopted an hyper-spectral scanner. This scanner has been designed and assembled at the N. Carrara Institute of Applied Physics of the Italian Research Council (IFAC-CNR).¹⁶ It has a spatial sampling step of 0.1 mm and spectral sampling step of about 1 nm. The spectral range acquirable lies between 400 and 900 nm. This instrument is based on the transmission spectrograph ImSpector Prism-Grating-Prism made by SpecIm Ltd. A calibrated and certified Spectralon[®] 99% was used as the white reference diffuser for the calibration. The scanning of an object produces a digital image (called “cube”) in which every pixel exhibits the reflectance spectrum of the corresponding point of the object measured. From these spectra CIELAB values are derived.

The availability of the whole CIELAB image of the object solves the problem of the validation of the proposed methodology, allowing the possibility of evaluating the colorimetric error (ΔE) for all the pixels. However, this approach implies a burdensome pixel-to-pixel geometric registration necessary to obtain the correspondence between the pixels in the image derived from the hyper-spectral scanning and those in the RGB image acquired with a color imaging device (either scanner or digital camera). The issue is not trivial, considering that the acquisition set-ups are inevitably different.

For this reason, in this article, the RGB image was obtained from the cube through calculations, rather than by using a digital camera.

The “Mathematical” RGB Image

The RGB image was obtained by using the tabulated spectral sensitivities of a high-end digital single-lens reflex (DSLR) camera.^{17,18} The RGB image, in fact, was derived from processing [Eqs. (1), (2) and (3)] the reflectances

$R\%(\lambda)$ of the hyper-spectral image, taking the D50 lighting conditions into consideration.

$$R = \int_{380}^{780} D50(\lambda)R\%(\lambda)r(\lambda)d\lambda, \quad (1)$$

$$G = \int_{380}^{780} D50(\lambda)R\%(\lambda)g(\lambda)d\lambda, \quad (2)$$

$$B = \int_{380}^{780} D50(\lambda)R\%(\lambda)b(\lambda)d\lambda. \quad (3)$$

This way, the RGB image has the identical spatial sampling as the cube and, therefore, no geometric registration process is needed for the computation of the colorimetric error.

After we explain how to obtain the data, the whole methodology is described in the “Description of the Proposed Methodology” section.

DESCRIPTION OF THE PROPOSED METHODOLOGY

Let us suppose that we have a quasiplane object (e.g., a paper document, a photographic print, a fabric, a painting on canvas, etc.) and its RGB digital reproduction. The methodology presented here seeks the color accuracy of the reproduction. As already stated in the Introduction, the colorimetric accuracy will be considered here. According to the diagram in Figure 1, the methodology is divided into different operating blocks that are described in the following subsections.

Finding the Training Set

The first operational block identifies, in the device-dependent space, the colors that better represent those of the object; in order to do that, the *k-means* algorithm¹⁹ has been applied to the three-dimensional RGB space. Among the advantages of this clustering algorithm, are simplicity, wide diffusion and the ability of setting the number of clusters. Unfortunately, the final result depends on the initial random partition chosen.

The *k* centroids $\{RGB_i^*\}$ ($i=1\dots k$) found by this procedure are the representative colors of the image. Since their values are not necessarily present in the image, the second operational block searches in the digital image, for each centroid, the pixel whose RGB triplet minimizes the 2-norm distance from the centroid itself. Each of these RGB triplets is then bound to its corresponding CIELAB triplet derived from the spectra measured by the hyper-spectral scanner. Thus, the two sets of *k* elements are in bijective correspondence: the first ($\{RGB_i\}$) in the device-dependent space and the second ($\{CIELAB_i\}$) in the device-independent space. Starting from these two sets it is possible to calculate the parameters of a transformation from the device-dependent space to the device-independent space.

Polynomial Modeling

In order to obtain this transformation, it is necessary to define, for each RGB_i triplet, a vector, whose terms are

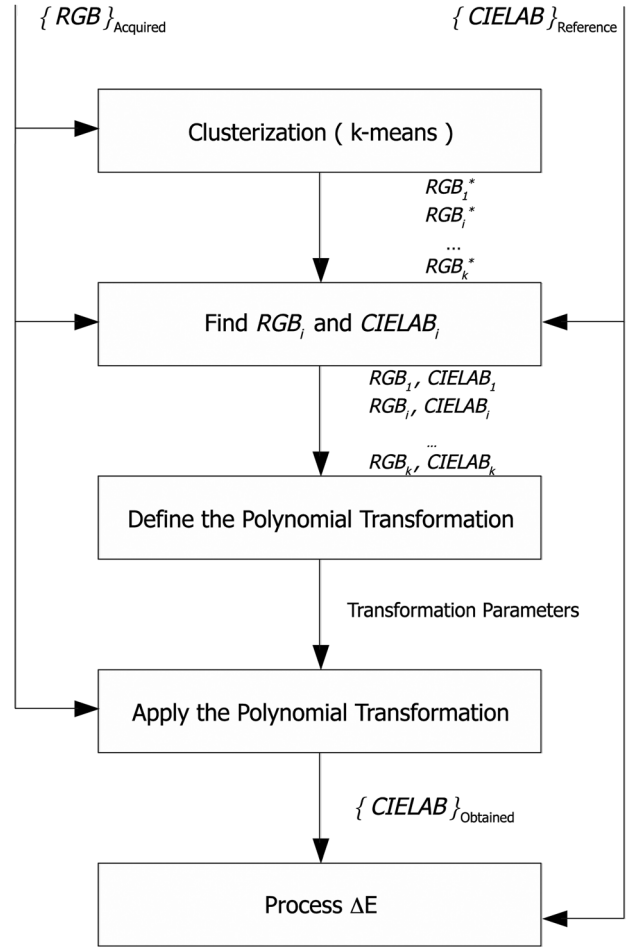


Figure 1. Block diagram describing the procedure proposed in this work.

composed by specific polynomial combination of *R*, *G*, and *B* values. Obviously, there are unlimited possibilities to combine these values polynomially; however, following what the literature⁵ proposes, the choice was limited to the third order terms. In this way, considering all possible terms, each RGB_i triplet determines a vector \mathbf{v}_i of dimension 1×20 . Since the set $\{RGB_i\}$ is composed by *k* elements, it is possible to define a matrix **A** of size $k \times 20$, where each row is \mathbf{v}_i . Each row is a nonlinear combination of the corresponding RGB triplet. Table I shows the most frequent polynomial combinations adopted in the literature and the relative size of the matrix **A**; this work uses the one in the last row. Furthermore, let **b** be the $k \times 3$ matrix

Table I. Polynomial combinations adopted in the literature.

A	Row value
$k \times 3$	[R G B]
$k \times 4$	[1 R G B]
$k \times 5$	[1 R G B RGB]
$k \times 10$	[1 R G B RG RB GB R ² G ² B ²]
$k \times 20$	[1 R G B RG RB GB R ² G ² B ² RGB R ² G R ² B G ² R G ² B B ² R B ² G R ³ G ³ B ³]

where each row is a triplet of the set $\{CIELAB_i\}$. The transformation adopted is defined by the 20×3 sized matrix \mathbf{x} that maximizes the residues

$$\| \mathbf{b}_j - \mathbf{A}\mathbf{x}_j \| \quad j = 1 \dots 3. \quad (4)$$

The symbol $\| \cdot \|$ indicates the Euclidean distance and the subscript j is the column of the matrix. For this reason, the matrix \mathbf{x} is the solution of the linear least squares problems (LLS). This classic problem can be solved by means of different approaches: in this experiment the SVD decomposition was adopted, because it provides the best guarantee of stability of the solution depending on the *machine epsilon*.²⁰

Since the matrix \mathbf{A} is composed by linear, quadratic, and cubic terms, it is ill-conditioned. In order to give preference to a particular solution with desirable properties, a regularization term can be included in this minimization. Choosing the Tikhonov regularization²¹ and giving preference to solutions with smaller norms, for each j -column the following quadratic convex optimization has to be processed:

$$\text{minimize } \| \mathbf{b}_j - \mathbf{A}\mathbf{x}_j \|^2 + \gamma \| \mathbf{x}_j \|^2, \quad (5)$$

where γ is a weight to balance the contribution of the two norms in Eq. (5). In the following experiments, γ is set to 0.5. The analytical solution of Eq. (5) is

$$\mathbf{x}_j = (\mathbf{A}^t \mathbf{A} + \gamma \mathbf{I})^{-1} \mathbf{A}^t \mathbf{b}_j. \quad (6)$$

Using the minimization defined by Eqs. (4) and (5), the reference colors $\{RGB_i\}$ ($i = 1 \dots k$) are optimally mapped to the set $\{CIELAB_i\}_{\text{Obtained}}$. Unfortunately, there is no way to choose the colors that will be mapped well and those that will be mapped poorly. To overcome this problem, some authors²² used the constrained least squares regression. The usage of this regression allows determination of the best least squares transformation subject to the constraint that one—or more—reference colors are mapped without error. $\{RGB_m\}$ ($m = 1 \dots h, h < k$) defines this subset of colors. Given the constraints, the new formulation of the problem (in the Tikhonov variant) is the following:

$$\begin{aligned} &\text{minimize } \| \mathbf{b}_j - \mathbf{A}\mathbf{x}_j \|^2 + \gamma \| \mathbf{x}_j \|^2 \\ &\text{subject to } \mathbf{A}_{m,:} \mathbf{x}_j - \mathbf{b}_{m,j} = 0 \quad \text{for } m = 1, \dots, h, \end{aligned} \quad (7)$$

or, taking the machine epsilon into account:

$$\begin{aligned} &\text{minimize } \| \mathbf{b}_j - \mathbf{A}\mathbf{x}_j \|^2 + \gamma \| \mathbf{x}_j \|^2 \\ &\text{subject to } | \mathbf{A}_{m,:} \mathbf{x}_j - \mathbf{b}_{m,j} | \leq \delta \\ &\quad \text{for } m = 1, \dots, h \text{ and } \delta > 0, \end{aligned} \quad (8)$$

where $:$ indicates the whole row.

In the experiments reported below, the parameter δ is set to 10^{-1} .

Since the constraints in Eq. (7) are affine and those in Eq. (8) are convex, problems (7) and (8) are convex optimization problems.²³ Thus, these problems can be solved

using the software available at the CVX research site.²⁴ With adoption of this software, the implementation of the Lagrange multiplier method is no longer necessary.

Other authors²⁵ improved the general Tikhonov regularization by setting up a curvature penalization. Since the values $\{RGB_i\}$ are neither sorted nor arranged, this improvement is not useful in our case.

Evaluation of the Color Accuracy

Once the matrix \mathbf{x} has been found, each 1×20 vector \mathbf{v} , obtained from a single pixel of the image, is multiplied by the transposed matrix \mathbf{x}^t , thereby obtaining the corresponding CIELAB values. The image obtained in the CIELAB color space is the result of the color optimization. In order to evaluate the effectiveness of the color optimization, these values have to be compared with the measured CIELAB values. In this way, a map of the colorimetric error ΔE and its relative statistics are obtained. The mean of the ΔE for all the pixels of the image is considered to be the indicator of color accuracy.

EXPERIMENTS AND RESULTS

The experiment presented here aims at providing quantitative and qualitative information on the performance of the proposed methodology. As stated in the Introduction, when the chromatic content of the object that has to be reproduced is distributed within a limited volume of the color space, the general characterization of the acquisition device with standard color targets is particularly unsuitable.⁷ Accordingly, two monochromatic photographic prints were selected as the case study. The chosen prints belong to the Berenson archive, which is part of the Harvard University—Center for Italian Renaissance Studies. They are silver gelatin prints produced in the first decades of the 20th Century characterized by a classic sepia tone, obtained by toning treatment. In order to carry out a comparison between the proposed specific optimization and the general characterization, an IT8/7.2 chart was included in the scene. The presence of a fourth object in the scene acquired—a palette of 24 saturated colors—allowed us to assess the results of a specific polynomial transformation to an object whose color characteristics were totally different compared to those from which the transformation was derived (the sepia prints).

Figure 2 shows the acquired scene as the hyper-spectral scanner framed it.

In the discussion of results, *Photo-1* indicates the print on the left in Fig. 2; *Photo-2* indicates the print on the right; *Palette* indicates the palette of 24 saturated colors.

In order to assess the performance of the procedure, each photographic print was used as a separate input for the methodology, and we evaluated the results adopting the values $\{24, 30, 60, 140\}$ for factor k (number of reference colors): 24 is the number of patches of the ColorChecker[®], 140 is the number of patches of the ColorChecker[®] SG, 60 is actually the number of colors suggested in the literature¹² as the optimal for polynomial modeling.



Figure 2. The image of the objects acquired by the hyper-spectral scanner.

In order to assess the methodology when the minimization is subject to constraints, it is necessary to choose the colors of the subset $\{RGB_m\}$. Due to its importance, some authors²² choose one single color, the white reference. For our case of photographic prints, the unexposed photographic paper has to be considered as particularly significant. The unexposed paper could be labeled by more than one reference color of the training set. This is more likely when a high number of reference colors is used. However, selecting a small area of the paper, it is possible to find the corresponding reference colors.

By use of the IT8 color chart, the usual profiling procedure was carried out with the software PROFILEMAKER 5.0 and selection of the “Reproduction” option, as it does not numerically distort the camera signals to make the image more pleasant.²⁶ For calculation of the ICC profile, the PROFILEMAKER process refers to the reflectance spectra of the IT8 target; by default it refers to the tabulated data of the standard reflectances. In this case, to maximize the comparability, rather than the tabulated reflectance values of the IT8 the reference reflectance values input in PROFILEMAKER were those obtained from the measurements

performed on the target by the hyper-spectral scanner. The ICC profile obtained provided the CIELAB values of each point on the whole image.

A Preliminary Experiment

A first experiment was conducted in order to verify the degree of mismatch between the metamerism corresponding to a DSLR camera and the metamerism of the human visual system. Since the spectral sensitivities of the DSLR camera do not satisfy the Luther-Ives conditions, there exists a set of colors that the camera records with the same triplet RGB, but which does not have the same CIELAB reference values. In order to assess this mismatch, the RGB triplets inside the unitary cube that contains the centroid, found by k-means, are considered for each cluster of the image. Figure 3 reports the data corresponding to one of the clusters of *Photo-1* with $k=60$. In the graphs on top, the projections R-G, B-G, and B-R are shown. The plus sign indicates the coordinates of the centroid. The corresponding CIELAB values (scatter plots for L-a, L-b, and b-a projections) are reported in the bottom graphs. Observing

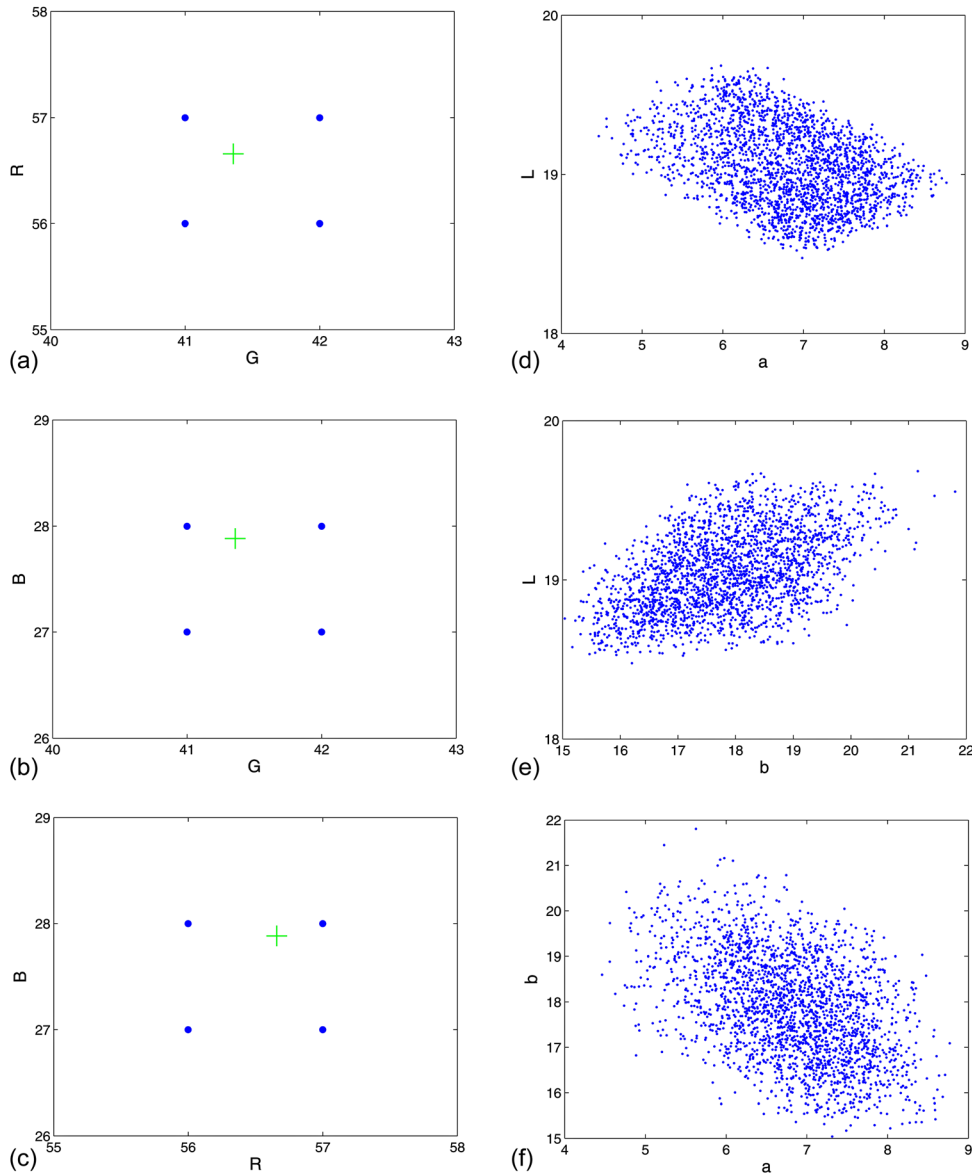


Figure 3. Effect of the metamer mismatch measured on one cluster of *Photo-1*.

the scatter plots of the corresponding CIELAB values, we see a significant spread along the L , a and b axes.

Discussion of the Results

First of all, the proposed methodology is assessed in the Tikhonov regularization framework. In order to do this, an experiment is conducted on *Photo-1*. The results are reported in Table II. Table II highlights that its average results are good only when the number of constraints is not high. When the number of reference colors is $k=140$, the results are not good: this is due to the increasing difficulty to satisfy the constraints. For this case, in fact, eight reference colors are identified in the unexposed paper and thus eight constraints have to be satisfied. Therefore, in consideration of the average results, there is no advantage in adopting it. For this reason, in the remaining part of the

paragraph we discuss only two variants of the proposed methodology: solving the minimization LLS problem and the convex quadratic problem in the form of the Tikhonov regularization.

Table II. Comparison among Tikhonov regularization with and without constraints: average ΔE obtained on *Photo-1*.

Number of reference colors	Tikhonov without constraints	Tikhonov with constraints	Number of constraints (unexposed paper)
24	1.12	1.12	1
30	1.11	1.11	2
60	0.84	0.86	3
140	0.71	3.64	8

Table III. Application of the proposed methodology: average ΔE obtained on *Photo-1*.

Number of reference colors	ICC profiling PROFILEMAKER	k-means and polynomial transformation	
		LLS	Tikhonov
252	3.09	—	—
24	—	29.13	1.12
30	—	7.50	1.12
60	—	1.04	0.84
140	—	0.73	0.71

Accordingly Tables III and IV show for different values of k the average colorimetric error calculated over all the pixels of each image after the application of the proposed methodology in the two variants for *Photo-1* and *Photo-2*, respectively. Tables III and IV reveal that Tikhonov variant clearly outperforms LLS variant. In both variants the average colorimetric error (ΔE) drops as the number of reference colors increases.

The presence of the regularization is important especially in case the number of reference colors is low. In fact, for $k=24$ and $k=30$, the Tikhonov regularization reduces the error dramatically. In Figure 4, for the case of *Photo-1* and $k=30$, the columns of the matrix x are plotted for both variants of the methodology. The remarkable effects of the regularization are evident.

Continuing analysis of the Tables III and IV, referring to LLS variant and $k=24$, we find that the high values of the average ΔE are due to the near coincidence between the number of coefficients of the polynomial transformation (20) and the present value of the k factor. In other words, since the model (the polynomial transformation with 20 coefficients) has too many degrees of freedom in relation to the number (24) of available data, a problem of overfitting arises. Accordingly a slight increase in k to 30, thus departing from the criticality of overfitting, the average ΔE is lowered considerably.

The same tables show also that the performance of the proposed specific methodology in both variants is definitely

Table IV. Application of the proposed methodology: average ΔE obtained on *Photo-2*.

Number of reference colors	ICC profiling PROFILEMAKER	k-means and polynomial transformation	
		LLS	Tikhonov
252	3.53	—	—
24	—	10.38	1.04
30	—	3.02	0.96
60	—	1.86	0.79
140	—	0.91	0.71

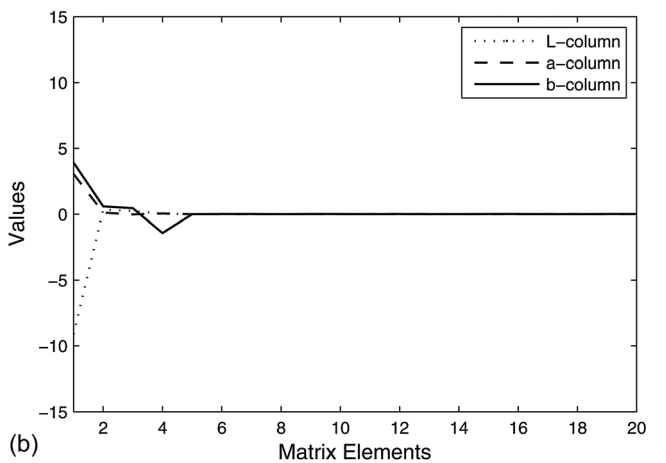
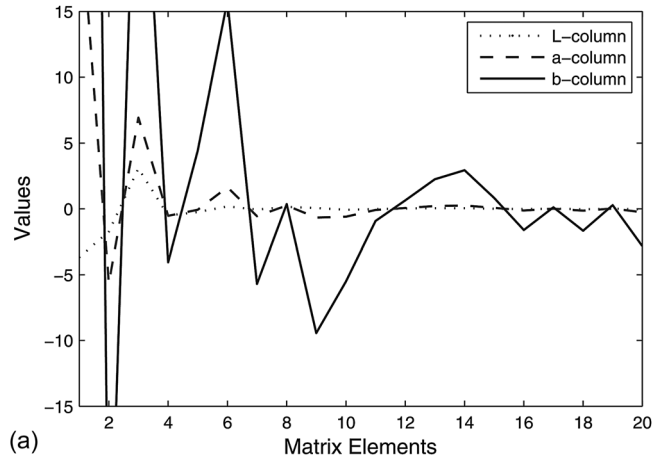


Figure 4. Plot of the values of x for *Photo-1*: values obtained by (a) LLS and (b) Tikhonov.

better than that obtained with the general profiling procedure. Moreover, if we consider that the general profiling procedure uses 252 reference colors, the benefits of the proposed procedure become even more evident. If one considers the LLS variant, the polynomial transformation exceeds the general profiling procedure only with a high number of reference colors. The proposed methodology in Tikhonov variant in every case largely outperform the profilation by PROFILEMAKER.

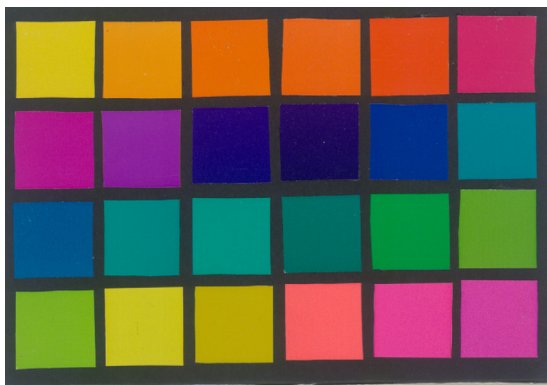
Another experiment involves *Palette* (see Figure 2, upper left quadrant). This experiment aims at highlighting some limits of the methodology proposed. Table V shows the colorimetric error found for *Palette*: first, after the application of the transformation found from a selection of colors performed on *Palette* itself, then, after the application the transformation specific for *Photo-2*. The application of the parameters of the polynomial transformation calculated on *Photo-2* to *Palette* (Table V) produces an average ΔE that is not acceptable. The correct application of the complete methodology to *Palette* determines an average ΔE of 1.39, thus confirming that the *Palette* scene does not show any particular problem. Figure 5 shows the images

Table V. Crash test: Average ΔE obtained on Palette with 60 reference colors.

Image on which color selection is performed	k-means and polynomial transformation	
	LLS	Tikhonov
Palette	1.39	1.39
Photo-2	174.77	28.74

obtained after the two transformations by using Tikhonov variant: the image (b) obtained from the polynomial transformation calculated on *Photo-2*, reveals colors that are dramatically incorrect.

Therefore, by selecting the significant colors of the object, the methodology presented here obtains the specificity that allows better performance but, at the same time, is applicable only to objects with similar color characteristics. In other words, this is the typical conflict between specificity and generality. In fact, if the polynomial transformation defined on a particular object is applied to another with completely different color characteristics, color accuracy may not be satisfactory.



(a)



(b)

Figure 5. sRGB images of Palette obtained by calculating the parameters of the polynomial transformation on Palette itself (a) or on *Photo-2* (b).

CONCLUSIONS

An object-specific methodology for the color optimization of a digital image has been presented. The training set used to perform the optimization, rather than being constituted by the traditional color targets, is a selection of points of the object that has to be reproduced.

With respect to the general colorimetric characterization that uses standard color targets, the methodology presented here has two main advantages that make the color optimization perform better:

- (1) The colorimetry of the training set reflects the Colorimetric characteristics of the object to be reproduced.
- (2) The match between the type of materials that constitute the training set and the type of materials that constitute the object to be reproduced is perfect.

The experiments numerically prove the effectiveness of the presented methodology, in particular when the Tikhonov regularization is adopted in the optimization process. An interesting result is that the methodology in its Tikhonov variant shows little sensitivity to the number of reference colors. Moreover, the study highlights the potential risks associated with improper use of the methodology.

For its application in operational contexts, when a hyper-spectral scanner is not necessary, a limited number of points can be considered by using a spot spectrophotometer. The issues and the problems related to the optimal selection of such a limited number of points will be the matter of future investigation.

ACKNOWLEDGMENTS

The authors wish to thank Andrea Casini and Marco Poggesi of the N. Carrara Institute of Applied Physics (CNR, Firenze) for their support during hyper-spectral acquisitions as well as the staff of the Berenson archive (Harvard University—Center for Italian Renaissance Studies) for their kind helpfulness.

REFERENCES

- ¹P.-C. Hung, "Colorimetric calibration in electronic imaging devices using a look-up table model and interpolations", *J. Electron. Imaging* **2**, 53 (1993).
- ²H. R. Kang, "Color scanner calibration," *J. Imaging Sci. Technol.* **36**, 162 (1992).
- ³H. R. Kang and P. G. Anderson, "Neural network applications to the color scanner and printer calibrations," *J. Electron. Imaging* **1**, 125 (1992).
- ⁴ISO 15076-1, 2005, "Image technology colour management—Architecture, profile format and data structure," ISO, Geneva, 2005 www.iso.org.
- ⁵V. Cheung and S. Westland, "Methods for optimal color selection," *J. Imaging Sci. Technol.* **50**, 481 (2006).
- ⁶Y. F. Chou, C. Li, and R. M. Luo, "A new colour selection method for characterizing digital cameras," *Proc. IS&T/SID 17th Color Imaging Conference (IS&T)*, Springfield, VA, 2009) pp. 75–78.
- ⁷G. Trumpy, "Digital reproduction of small gamut object: A profiling procedure based on custom color targets," *Proc. IS&T CGIV (IS&T)*, Springfield, VA, 2010) pp. 143–147.
- ⁸R. W. G. Hunt, *Measuring Colour*, 3rd ed. (Fountain Press, London, 1998).

- ⁹R. Gschwind and G. Di Pietro, "Metamerism in colour imaging systems and 'reverse' colour reproduction," *Proc. International Congress on Imaging Science ICPS 98* vol. 2, (International Committee on the Science of Photography, Antwerpen, 1998) pp. 11–14.
- ¹⁰H. E. Ives, "The transformation of color-mixture equations from one system to another," *J. Franklin Inst.* **16**, 673 (1915).
- ¹¹P. Urban and R. R. Grigat, "Metamer density estimated color correction," *Signal, Image Video Process.* **3**, 171 (2009).
- ¹²G. Hong, R. M. Luo, and P. A. Rhodes, "A study of digital camera colorimetric characterization based on polynomial modelling," *Color Res. Appl.* **26**, 76 (2001).
- ¹³J. Y. Hardeberg, "Acquisition and reproduction of colour images: Colorimetric and multispectral approaches," Ph.D. dissertation Ecole Nationale Supérieure des Télécommunications, Paris, 1999.
- ¹⁴M. Strgar Kurečić, D. Agić, and L. Mandić, "Color accurate imaging of artworks using custom color reference target for digital camera characterization," *Proc. 33rd IARIGAI International Research Conference (IARIGAI, Darmstadt, 2006)* pp. 361–367.
- ¹⁵S. Yamamoto, N. Tsumura, T. Nakaguchi, and Y. Miyake, "Development of a multi-spectral scanner using LED array for digital color proof," *J. Imaging Sci. Technol.* **51**, 61 (2007).
- ¹⁶M. Picollo, M. Bacci, A. Casini, F. Lotti, M. Poggessi, and L. Stefani, "Hyper-spectral image spectroscopy: A 2-D approach to the investigation of polychrome surfaces," *Proc. Conservation Science International Conference (Archetype, London, 2008)* pp. 162–168.
- ¹⁷See <http://www.image-engineering.de> for image engineering, "spectral sensitivities of several cameras (mainly SLR)", accessed October 2010.
- ¹⁸C. Mauer, "Measurement of the spectral response of digital cameras with a set of interference filters", Ph.D. dissertation (Fachhochschule, Köln, 2009).
- ¹⁹K. Fukunaga, *Introduction to Statistical Pattern Recognition*, 2nd ed. (Academic Press, Boston, MA, 1990).
- ²⁰L. N. Trefethen and D. Bau III, *Numerical Linear Algebra*, (Society for Industrial and Applied Mathematics, Philadelphia, PA, 1997).
- ²¹A. N. Tikhonov, "Solution of incorrectly formulated problems and the regularization method," *Sov. Math. Dokl.* **4**, 1035 (1963).
- ²²G. D. Finlayson and M. S. Drew, "Constrained least-squares regression in color space," *J. Electron. Imaging* **6**, 484 (1997).
- ²³S. Boyd and L. Vandenberghe, *Convex Optimization* (Cambridge University Press, Cambridge, UK, 2004).
- ²⁴See <http://www.cvr.com> for CVX research, "CVX: Matlab software for disciplined convex programming," accessed July 2011.
- ²⁵B. S. Dissing, J. M. Carstensen, and R. Larsen, "Multispectral colormapping using penalized least square regression," *J. Imaging Sci. Technol.* **54**, 030401 (2010).
- ²⁶P. Rao, M. R. Rosen, and R. S. Berns, "Performance evaluation of the Profile-Maker professional 5.0 ICC profiling software," Munsell Color Science Technical Report (2005), available at http://www.art-si.org/PDFs/Processing/TechnicalReportProfileMaker_05.pdf, accessed December 2011.